

Domain Adaptation As a Problem of Inference on Graphical Models

Kun Zhang^{1*} Mingming Gong^{2*} Petar Stojanov¹ Biwei Huang¹
 Clark Glymour¹

¹Carnegie Mellon University, Pittsburgh, PA 15213, USA

²University of Melbourne, Melbourne, Australia

Abstract

This paper is concerned with data-driven unsupervised domain adaptation, where it is unknown in advance how the joint distribution changes across domains, i.e., what factors or modules of the data distribution remain invariant or change across domains. To develop an automated way of domain adaptation with multiple source domains, we propose to use a graphical model as a compact way to encode the change property of the joint distribution, which can be learned from data, and then view domain adaptation as a problem of Bayesian inference on the graphical models. Such a graphical model distinguishes between constant and varied modules of the distribution and specifies the properties of the changes across domains, which serves as prior knowledge of the changing modules for the purpose of deriving the posterior of the target variable Y in the target domain. This provides an end-to-end framework of domain adaptation, in which additional knowledge about how the joint distribution changes, if available, can be directly incorporated to improve the graphical representation. We discuss how causality-based domain adaptation can be put under this umbrella. Experimental results on both synthetic and real data demonstrate the efficacy of the proposed framework for domain adaptation.

1 Introduction

Over the past decade, various approaches to unsupervised domain adaptation (DA) have been pursued to leverage the source-domain data to make prediction in the new, target domain. In particular, we consider the situation with n source domains in which both the d -dimensional feature vector X , whose j th dimension is denoted by X_j , and label Y are given, i.e., we are given $(\mathbf{x}^{(i)}, \mathbf{y}^{(i)}) = (\mathbf{x}_k^{(i)}, y_k^{(i)})_{k=1}^{m_i}$, where $i = 1, \dots, n$, and m_i is the sample size of the i th source domain. We denote by $x_{jk}^{(i)}$ the value of the j th feature of the k th data point (example) in the i th domain. Our goal is to find the classifier for the target domain, in which only the features $\mathbf{x}^\tau = (\mathbf{x}_k^\tau)_{k=1}^m$ are available. Because the distribution may change across domains, clearly the optimal way of adaptation or transfer depends on what information is shared across domains and how to do the transfer.

In the covariate shift scenario, the distribution of the features, $P(X)$, changes, while the conditional distribution $P(Y|X)$ remains fixed. A common strategy is to reweight examples from the source domain to match the feature distribution in the target domain—an approach extensively studied in machine learning; see e.g., [46, 56, 21, 52, 3, 9]. A common prerequisite for such an approach is that the support for the source domain include the target domain, but of course this is often not the case. Another collection of methods learns a domain-invariant feature representation that has identical distributions across the target and source domains [35, 1, 15, 28, 12].

In addition, it has been found that $P(Y|X)$ usually changes across domains, in contrast to the covariate shift setting. For the purpose of explaining and modeling the change in $P(Y|X)$, the

*equal contribution

problem was studied from a generative perspective [51, 45, 60, 57, 41]—one can make use of the factorization of the joint distribution corresponding to the causal representation and exploit how the factors of the joint distribution change, according to commonsense or domain knowledge. The settings of target shift [51, 41, 60, 22, 26] and conditional shift [60, 31, 29] assume only $P(Y)$ and $P(X|Y)$ change, respectively, and their combination, as generalized target shift [60, 7], was also studied, and the corresponding methods clearly improved the performance on a number of benchmark datasets. The methods were extended further, by learning feature representations with invariant conditionals given the label and matching joint distributions [31, 30, 10], and it was shown how methods based on domain-invariant representations can be understood from this perspective.

How are the distributions in different domains related? Essentially, DA aims to discover and exploit the constraints in the data distribution implied by multiple domains and make prediction that adapts to the target domain. To this end, we assume that the distributions of the data in different domains were independent and identically distributed (I.I.D.) drawn from some “mother” distribution. The mother distribution encodes the uncertainty in the domain-specific distributions, i.e., how the joint distribution is different across the domains. Suppose the mother distribution is known, from which the target-domain distribution is drawn. Furthermore, the target domain contains data points (without Y values) generated by this distribution. It is then natural to leverage both the mother distribution and the target-domain feature values to reveal the property of the target-domain distribution for the purpose of predicting Y . In other words, DA is achieved by exploiting the mother distribution and the target-domain feature values to derive the information of Y .

Following this argument, we have several questions to answer. First, is there a natural, compact description of the constraints on the changes of the data distribution (to describe the mother distribution)? Such constraints include which factors of the joint distributions can change, whether they change independently, and the range of changes. (We represent the joint distribution as a product of the factors.) Second, how can we find such a description from the available data? Third, how can we make use of such a description as well as the target-domain data to make optimal prediction? Traditional graphical models have provided a compact way to encode conditional independence relations between variables and factorize the joint distribution [37, 23]. We will use an extension of Directed Acyclic Graphs (DAGs), called augmented DAGs, to factorize the joint distribution and encode which factors of the joint distribution change across domains. The augmented DAG, together with the conditional distributions and changeability of the changing modules, gives an augmented graphical model as a compact representation of how the joint distribution changes. Predicting the Y values in the target domain is then a problem of Bayesian inference on this graphical model given the observed target-domain feature values. This provides a natural framework to address the problem of DA in an automated, end-to-end manner.

It is worth noting that the graphical model we use to describe the mother distribution is not necessarily a causal model. The observed data were generated by the underlying generating (causal) process and then the sampling process (which samples data from the population to produce the observed data). Recovering the underlying causal structure from the observed data is in general rather challenging; on the other hand, as long as the property of the mother distribution regarding how the joint distribution changes across domains can be recovered and applied to the target domain, DA can be achieved. Our graphical model simply provides a compact representation of the mother distribution, which can be estimated from data in different domains in a rather straightforward way. In many tasks such as estimating causal effects [43, 38] or determining transportability of experimental findings [39], one has to use causal models. However, for our purpose it suffices to use our graphical model; As discussed in Section 2.2, our graphical structure may be very different from the causal structure.

2 DA and Inference on Graphical Models

We start with a brief review of existing methods for unsupervised DA and then present the proposed idea of performing DA as an inference problem on graphical models. In this section we assume that the graphical model for describing the distribution change across domains is given, and how to

implement the idea from the given domain data is discussed in the next section.

2.1 Domain Adaptation

Unsupervised DA aims to construct the classifier for the target domain, on which only the features $\mathbf{x}^\tau = (x_k^\tau)_{k=1}^m$ are available, by making proper use of the data in s source domains $(\mathbf{x}^{(i)}, \mathbf{y}^{(i)}) = (\mathbf{x}_k^{(i)}, y_k^{(i)})_{k=1}^{m_i}$, $i = 1, \dots, s$. Here we are concerned with the scenario where no labeled point is available in the target domain, known as unsupervised DA. To make successful prediction in the target domain, there must exist relevant knowledge to transfer to the target domain. Various assumptions on how distribution changes were proposed to make successful knowledge transfer possible. For instance, a classical setting assumed that $P(X)$ changes but $P(Y|X)$ remains the same, i.e., the covariate shift situation; see, e.g., [46, 21, 52, 3]. It is also known as sample selection bias (particularly on the features X) in [56]. The correction of shift in $P(X)$ can be achieved by re-weighting source domain examples using importance weights as a function of feature X [46, 52, 21, 9], based on certain distribution discrepancy measures such as Maximum Mean Discrepancy (MMD) [19]. Another collection of methods learns a domain-invariant representation by applying suitable linear transformation or nonlinear transformation or by properly sampling, which has identical distributions across the target and source domains [35, 1, 15, 28, 12].

In practice it is very often that both P_X and $P_{Y|X}$ change simultaneously across domains. For instance, both of them are likely to change over time and location for a satellite image classification system. If the data distribution changes arbitrarily across domains, clearly knowledge from the sources may not help in predicting Y in the target domain [44]. One has to find what type of information should be transferred from sources to the target. A number of works are based on the factorization of the joint distribution as $P_{XY} = P_{X|Y}P_Y$, in which either change in P_Y or in $P_{X|Y}$ will cause changes in both P_X and $P_{Y|X}$ according to the Bayes rule. One possibility is to assume the change in both P_X and $P_{Y|X}$ is due to the change in P_Y , while $P_{X|Y}$ remains the same, as known as prior probability shift [51, 41] or target shift [60]. Similarly, one may assume conditional shift, in which P_Y remains the same but $P_{X|Y}$ changes [60]. In practice, target shift and conditional shift may both happen, which is known as generalized target shift.

Various methods have been proposed to deal with the above situations. Target shift can be corrected by re-weighting source domain examples using an importance function of Y , which can be estimated by density matching [60, 22, 26]. Conditional shift is in general ill-posed because without further constraints on it, $P^\tau(X|Y)$ is generally not identifiable given the source-domain data and the target-domain feature values. It has been shown to be identifiable when $P(X|Y)$ changes in some parametric ways, e.g., when $P_{X|Y}$ changes under location-scale transformations of X [60]. In addition, the invariant representation learning methods originally proposed for covariate shift can be adopted to achieve invariant causal mechanism [16]. Pseudo labels in the target domain may be exploited to refine the matching of conditional distributions [29, 55]. Finally, generalized target shift has also been addressed by joint learning of domain-invariant representations and instance weighting function; see e.g., [60, 16, 7].

For the purpose of discover what to transfer in a automated way, in this paper we *mainly consider DA with at least two source domains*, although the method can be applied to the single-source case if proper additional constraints are known—for instance, in DA from the MNIST data (a single source code) to the USPS data, as studied in Subsection 5.1, we know that the distribution of the class label, $P(Y)$, remains unchanged, which makes it possible to do the transfer with a single source domain. Generally speaking, the availability of multiple source domains provides more hints helpful to find $P_{X|Y}^t$ as well as $P_{Y|X}^t$. Several algorithms have been proposed to combine knowledge from multiple source domains. For instance, they combine source hypotheses with a distribution weighted rule to form the target hypothesis [33], or combine the predictions made by the source hypotheses with the weights determined in different ways [13, 11, 6]. As one may see, existing methods mainly assume the properties of the distribution shift and utilize the assumptions for DA; furthermore, the involved assumptions are usually rather strong. Violation of the assumptions may lead to negative transfer.

An essential question then naturally arises—is it possible to develop a data-driven approach to

automatically figure out what information to transfer from the sources to the target and make optimal prediction in the target domain, under mild conditions? This paper aims at an attempt to answer this question, by representing the properties of distribution change with a graphical model, estimating the graphical model from data, and treating prediction in the target domain as a problem of inference on the graphical model given the target-domain feature values. Below we present the used graphical models and how to use them for DA.

2.2 Describing Distribution Change Properties with Augmented Graphical Models

In the target domain, the Y values are to be predicted, and we aim at their optimal prediction with respect to the joint distribution. To find the target-domain distribution, one has to leverage source-domain data and exploit the connection between the distributions in different domains. It is then natural to factorize the joint distribution into different components or modules—it would facilitate recovering the target distribution if as few components as possible change across the domains (i.e., as many components as possible remain invariant). Furthermore, in estimation of the changing modules in the target domain, it will be beneficial if those changes are not relevant to each other so that one can do “divide-and-conquer”; otherwise, if the changes are coupled, one has to estimate the changes together and would suffer from “curse-of-dimensionality.” In other words, DA benefits from a compact description of how the data distribution can change across domains—such a description, together with the given feature values in the target domain, helps recover the target joint distribution and enables optimal prediction. In this section we introduce our graphical model as such a way to describe distribution changes.

Traditional graphical models provide a compact, yet flexible, way to decompose the joint distribution of as a product of simpler, lower-dimensional factors [40, 23], as a consequence of conditional independence relations between the variables. In particular, if the conditional independence relations can be presented by a Directed Acyclic Graph (DAG), then the joint distribution can be factorized as the product of factors, each of which corresponds to the conditional distribution of a variable given its parents. For our purpose, we need encode not only conditional independence relations between the variables, but also whether the conditional distributions change across domains. To this end, we propose an augmented DAG as a flexible yet compact way to describe how a joint distribution changes across domains, assuming that the distributions in all domains can be represented by such a graph (in other words, this graph encodes the property of the mother distribution behind the domain-specific distributions). It is an augmented graph in the sense that it is over not only features X_i and Y , but also external latent variables θ .

Figure 1 gives an example of such a graph. Nodes in gray are in the Markov Blanket (MB) of Y . The θ variables are mutually independent, and take the same value across all data points within each domain and may take different values across domains. They indicate the property of distribution shift—for any variable with a θ variable directly into it, its conditional distribution given its parents (implied by the DAG over X_i and Y) depends on the corresponding θ variable, and hence may change across domains. In other words, the distributions across domains differ only in the values of the θ variables. Once their values are given, the domain-specific joint distribution is given by $P(\mathbf{X}, Y | \theta)$, which can be factorized according to the augmented DAG. In the example given in Figure 1, distribution factors $P(X_1)$, $P(Y|X_1)$, and $P(X_3|Y, X_2)$, among others, change across domains, while $P(X_5|Y)$ and $P(X_7|X_3)$ are invariant. The joint data distribution in the i th domain can be written as

$$P(\mathbf{X}, Y | \theta^{(i)}) = P(X_1 | \theta_1^{(i)}) P(Y | X_1, \theta_Y^{(i)}) P(X_5 | Y) P(X_2 | Y, X_4, \theta_2^{(i)}) P(X_3 | Y, X_2, \theta_3^{(i)}) \times \\ P(X_4) P(X_6 | X_4, \theta_6^{(i)}) P(X_7 | X_3).$$

We have several remarks to make on the used augmented graph. First, since the θ_i are independent, the corresponding conditional distributions change independently across domains. Because of such a

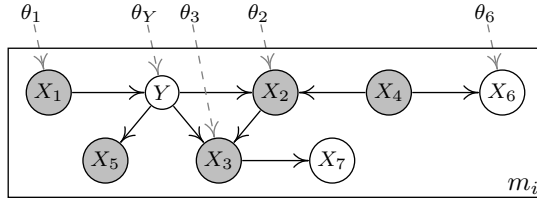


Figure 1: An augmented DAG over Y and X_i . See main text for its interpretation.

independence property, one can model and learn the changes in the corresponding factors separately. Second, we note that each node in the augmented graph may be a set of variables, as a “supernode” instead of a single one. (In the terminology of chain graphs, which have both directed and undirected edges, such a “supernode” can be considered as a chain component of the chain graph [24], and the joint distribution can be factorized as a “DAG of chain components”.) For instance, for the digit recognition problem, one can view the pixels of the digit image as such a “supernode” in the graph. Finally, as discussed above, for the purpose of predicting Y , we only need to exploit the conditional distributions of Y and its children. Hence, in practice one may not need to find the whole graph over all features and Y . This observation may accelerate the procedure of learning the augmented graph, which will be discussed in Section 3.1.

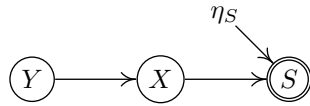
2.2.1 Relation to Causal Graphs

If the causal graph underlying the observed data is known, there is no confounder (hidden common cause of two variables), and the observed data are perfect random samples from the populations implied by the causal model, then one can directly benefit from using the causal model for transfer learning, as shown in [36, 60, 32]. In fact, in this case our graphical representation encodes the same conditional independence relations as the original causal model.

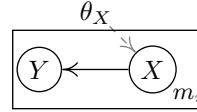
However, we emphasize that the graph we use for domain adaptation *is not necessarily a causal graph*. It is worth noting that the causal model, on its own, might not be sufficient to explain the properties of the data, for instance, because of selection bias [2], which is often present in the sample. Furthermore, it is *notoriously difficult to find causal relations* based on observational data; to achieve it, one often has to make rather strong assumptions on the causal model (such as faithfulness [49]) and sampling process. On the other hand, it is relatively easy to find the graphical model purely *as a description of conditional independence relationships* in the variables as well as the properties of changes in the distribution modules.

The underlying causal structure may be very different from the augmented DAG we adopt. Here we give two simple examples to illustrate the possible difference between the underlying causal structure and the graph we use for domain adaptation. In Example 1, let Y be disease and X the corresponding symptoms. It is natural to have Y as a cause of X . Suppose we have data collected in different clinics, each of which corresponds to a domain. Further assume that subjects are assigned to different clinics in a probabilistic way according to how severe the symptoms are. Figure 2(a) gives the causal structure together with the sampling process to generate the data in each domain. S is a selection variable, and a data point is selected if and only S takes value 1. $P(S = 1|X)$ depends on η_S , which may take different values across domains, reflecting different sampling mechanisms (e.g., subjects go to different clinics according to their symptoms). In this case, according to data in different domains, $P(X)$ changes. But $P(Y|X)$ will stay the same because according to the process given in (a), Y and S are conditionally independent given X and, as a consequence, $P(Y|X, S) = P(Y|X)$. The graphical model for describing the distribution change across domains is given in 2(b)—they are apparently inconsistent, and the direction between Y and X is reversed; however, for the purpose of DA, the graph in (b) suffices and, furthermore, as shown later, it can be directly learned from data from multiple domains.

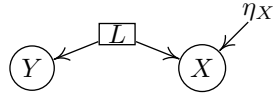
Example 2 follows the causal structure given in Figure 2(c), where X and Y are not directly causally related but have a hidden direct common cause (confounder) L and the generating process



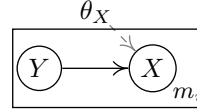
(a) The underlying data generating process of Example 1. Y generates (causes) X , and S denotes the selection variable (a data point is included if and only if $S = 1$).



(b) The augmented DAG representation for Example 1 to explain how the data distribution changes across domains.



(c) The generating process of Example 2. L is a confounder; the mechanism of X changes across domains, as indicated by η_X .



(d) The augmented DAG representation for Example 2 to explain how the data distribution changes across domains.

Figure 2: Two examples to illustrate the difference between the underlying causal graph and the augmented DAG used to represent the property of distribution changes across domains. (a) and (c) are the causal graphs of the two examples, and (b) and (d) the corresponding augmented DAGs.

of X also depends on η_X , which value may vary across domains. We care only about how the distribution changes—since in this example $P(Y)$ remains the same across domains, we can factorize the joint distribution as $P(Y, X) = P(Y)P(X|Y)$, in which only $P(X|Y)$ changes across domains, and the corresponding augmented DAG is shown in (d).

2.3 Inference on Augmented Graphical Models for DA

We now aim to predict the value (or the distribution) of Y given the observed features \mathbf{x}^τ in the target domain, which is about $P(\mathbf{Y}^\tau | \mathbf{x}^\tau)$, where \mathbf{Y}^τ is the concatenation of Y across all data points in the target domain. To achieve so, we have several issues to address. First, which features should be included in the prediction/inference procedure? Second, as illustrated in Figure 1, a number of distribution factors change across domains, indicated by the links from the θ variables, and it is not necessary to consider all of them for the purpose of DA—which changing factors should be adapted to the target-domain data? Third, for all data in the same domain the θ variables take the same value. It is then necessary to properly take into account this “parameter sharing” property in the inference procedure.

Let us first show the general results on calculation of $P(\mathbf{Y}^\tau | \mathbf{x}^\tau)$, based on which prediction in the target domain is made. We then discuss how to simplify the estimator, thanks to the specific augmented graphical structure over \mathbf{X} and Y . As the data are I.I.D. given the values of θ , we know $P(\mathbf{x}, \mathbf{y} | \theta) = \prod_k P(\mathbf{x}_k, y_k | \theta)$ and $P(\mathbf{x} | \theta) = \prod_k P(\mathbf{x}_k | \theta)$. Also bearing in mind that the value of θ is shared within the same domain, we have

$$\begin{aligned} P(\mathbf{Y}^\tau = \mathbf{y}^\tau | \mathbf{x}^\tau) &= \frac{P(\mathbf{y}^\tau, \mathbf{x}^\tau)}{P(\mathbf{x}^\tau)} = \frac{\int P(\mathbf{y}^\tau | \mathbf{x}^\tau, \theta) P(\mathbf{x}^\tau, \theta) d\theta}{\int \prod_k P(\mathbf{x}_k^\tau | \theta) P(\theta) d\theta} \\ &= \int \prod_k P(y_k^\tau | \mathbf{x}_k^\tau, \theta) \frac{\prod_k [\sum_{y_k^\tau} P(\mathbf{x}_k^\tau, y_k^\tau | \theta) P(\theta)]}{\int \prod_k [\sum_{y_k^\tau} P(\mathbf{x}_k^\tau, y_k^\tau | \theta)] P(\theta) d\theta} d\theta. \end{aligned}$$

For computational efficiency, we make prediction separately for different data points based on

$$P(y_k^\tau | \mathbf{x}^\tau) = \sum_{y_{k'}^\tau, k' \neq k} P(\mathbf{y}^\tau | \mathbf{x}^\tau) = \int P(y_k^\tau | \mathbf{x}_k^\tau, \theta) \frac{\prod_k [\sum_{y_k^\tau} P(\mathbf{x}_k^\tau, y_k^\tau | \theta)]}{\int \prod_k [\sum_{y_k^\tau} P(\mathbf{x}_k^\tau, y_k^\tau | \theta)] P(\theta) d\theta} d\theta. \quad (1)$$

In the above expression, $P(\theta)$ is given in the augmented graphical model, $P(y_k^\tau, \mathbf{x}_k^\tau | \theta)$ can be calculated by making use of the chain rule on the augmented graphical model, and $P(y_k^\tau | \mathbf{x}_k^\tau, \theta)$ can be estimated by training a probabilistic classifier on the generated data from our model.

Moreover, for the purpose of predicting Y , not all X_j are needed for the prediction of Y , and not all changing distribution modules need to adapt to the target domain. We exploit the graph structure to simplify the above expression. Let $\mathbf{V} = \mathbb{C}\mathbb{H}(Y) \cup \{Y\}$, where $\mathbb{C}\mathbb{H}(Y)$ denotes the set of children of Y relative to the considered augmented DAG. Also denote by $\mathbb{P}\mathbb{A}(V_j)$ the parent set of V_j . The conditional distribution of V_j given its parents is $P(V_j | \mathbb{P}\mathbb{A}(V_j), \theta_{V_j})$, where θ_{V_j} is the empty set if this conditional distribution does not change across domains. Let

$$\mathcal{C}_{jk} := P(v_{jk}^\tau | \mathbb{P}\mathbb{A}(v_{jk}^\tau), \theta_{V_j}) \quad (2)$$

be shorthand for the conditional distribution of V_j taking value v_{jk}^τ conditioning on its parents taking the k th value in the target domain and the value of θ_{V_j} . $P(\mathbf{x}_k^\tau, y_k^\tau | \boldsymbol{\theta})$ can be factorized as

$$P(\mathbf{x}_k^\tau, y_k^\tau | \boldsymbol{\theta}) = \left[\prod_{V_j \in \mathbf{V}} \mathcal{C}_{jk} \right] \cdot \underbrace{\left[\prod_{W_j \notin \mathbf{V}} P(w_{jk}^\tau | \mathbb{P}\mathbb{A}(w_{jk}^\tau), \theta_{W_j}) \right]}_{\triangleq N_k, \text{ which does not depend on } y_k^\tau}.$$

Substituting the above expression into Eq. 1, one can see that N_k , defined above, will not appear in the final expression, so finally

$$P(y_k^\tau | \mathbf{x}^\tau) = \int P(y_k^\tau | \mathbf{x}_k^\tau, \boldsymbol{\theta}) \frac{\prod_k [\sum_{y_k^\tau} \prod_{V_j \in \mathbf{V}} \mathcal{C}_{jk}] \prod_{V_j \in \mathbf{V}} P(\theta_{V_j})}{\int \prod_k [\sum_{y_k^\tau} \prod_{V_j \in \mathbf{V}} \mathcal{C}_{jk}] \prod_{V_j \in \mathbf{V}} P(\theta_{V_j}) d\boldsymbol{\theta}} d\boldsymbol{\theta}. \quad (3)$$

It is natural to see from the above final expression of $P(y_k^\tau | \mathbf{x}^\tau)$ that 1) only the conditional distributions for Y and its children (variables in \mathbf{V}) need to be adapted (their corresponding $\boldsymbol{\theta}$ variables are involved in the expression) and that 2) among all features, only those in the MB of Y are involved in the expression. Practical implementations of the estimation method will be discussed in Section 3.3.

2.3.1 Benefits from a Bayesian Treatment

Many traditional procedures for unsupervised DA are concerned with the identifiability of the joint distribution, or more specifically, the conditional distribution of the target given the features, in the target domain, where only feature values are given [36, 60, 16]. If the joint distribution is identifiable, a classifier can be learned by minimizing the loss with respect to the target-domain joint distribution. The work [36] considered the transportability of a particular quantity, the causal effects of one variable on another in a causal model, with graphical criteria. In the context of domain adaptation, it was shown that additional parametric constraints on the conditional distributions, e.g., the assumptions of location-scale transformations for the features given the label Y , help improve the identifiability of the target-domain joint distribution [60]. Without the identifiability of the relevant distributional information, successful DA is not guaranteed.

However, we note that even in the situation where the target-domain joint distribution (or the quantity of interest) is not identifiable, the Bayesian treatment, by incorporating the prior distribution of $\boldsymbol{\theta}$ and inferring the posterior of Y in the target domain, may provide very informative prediction—the prior distribution of $\boldsymbol{\theta}$ constrains the changeability of the distribution modules, and such constraints may enable “soft” identifiability of Y . We use an example to illustrate it. For clarity purposes, we use simple parametric models and a single feature X for the conditional distributions: $Y \sim \mathcal{N}(0, \theta_Y)$, $X = Y + E$, where $E \sim \mathcal{N}(0, \theta_X)$, i.e., $X|Y \sim \mathcal{N}(Y, \theta_2)$. So θ_Y controls the distribution of Y , and θ_X controls the conditional distribution of X given Y . The marginal distribution of X is then $X \sim \mathcal{N}(0, \theta_Y + \theta_X)$, which is what we can observe in the target domain. Clearly, from $P(X)$ in the target domain, $P(Y)$ or $P(X|Y)$ is not identifiable because $P(X)$ gives only $\theta_Y + \theta_X$. Now suppose we have prior distributions for θ_Y and θ_X : $\theta_Y \sim \Gamma(3, 1)$ and $\theta_X \sim \Gamma(1.5, 1)$, where the two arguments are the shape and scale parameters of the gamma distribution, respectively. Figure 3(a) shows their prior distributions, and (b) gives the corresponding posterior distribution of θ_Y given the variance of X , whose empirical version is observed in the target domain. One can see that although θ_Y as well as

θ_X is not theoretically identifiable, $P(\theta_Y | \text{Var}(X))$ is informative as to the value that θ_Y may take. Especially when $\text{Var}(X)$ is relatively small, the posterior distribution is narrow. The information we have about θ_Y and X then allows non-trivial prediction of the target-domain joint distribution and the Y values from the values of X .

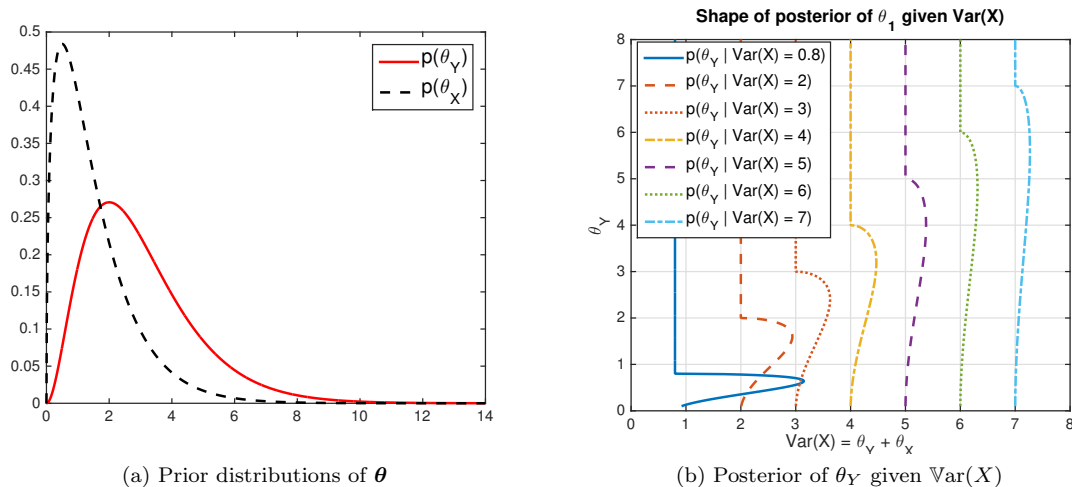


Figure 3: An illustration of the benefit of Bayesian treatment of the changeability of distribution modules (represented by the θ variables).

3 Implementation of Data-Driven DA

In practice we are given data and the graphical model is not available. For DA, we then need to learn (the relevant part of) the augmented graphical model from data, which includes the augmented DAG structure, the conditional distribution of each variable in $\mathbb{C}\mathbb{H}(Y) \cup \{Y\}$ given its parents, and the prior distribution of the relevant θ variables, and then develop computational methods for inferring Y on it given the target-domain data.

3.1 Learning the Augmented DAG

For wide applicability of the proposed DA procedure, we aim to find a nonparametric method to learn the augmented DAG, instead of assuming restrictive conditional models such as linear ones. We note that in the causality community, finding causal relations from nonstationary or heterogeneous data has attracted some attention in recent years. In particular, under a set of assumptions, a nonparametric method to tackle this causal discovery problem, called Causal Discovery from NONstationary/heterogeneous Data (CD-NOD) [58, 20], was recently proposed. The method is an extension of the PC algorithm [50] and consists of 1) figuring out where the causal mechanisms (or the corresponding conditional distributions) change, 2) estimation of the skeleton of the causal graph (i.e., edges of the causal graph but without directionality), and 3) determination of causal directions based on not only the orientation rules of the PC algorithm, but also the independent change property of causal modules (corresponding to distribution factors). Here we adapt their method for learning the portion of the augmented DAG that is needed for DA, without resorting to the assumptions made in their work. Denote by \mathbf{S} the set of Y and all X_i . The adapted method has the following three steps.

Step 1 (Finding changing distribution factors and estimating undirected graph) Let C be the domain index. Apply the first stage of the PC algorithm to $\mathbf{S} \cup \{C\}$ (the domain index C is

added to the variable set to capture the changeability of the conditional distributions); it starts with an undirected, fully connected graph, removes the edge between two variables that are conditionally independent given some other variables, and finally determines the skeleton. It is interesting to note that if variable $S_i \in \mathbf{S}$ is adjacent to C , then S_i is conditionally dependent on C given *any* subset of the remaining variables, and hence, there exists two different values of C , c_1 and c_2 , such that $P(S_i | \mathbb{P}\mathbb{A}(S_i), C = c_1) \neq P(S_i | \mathbb{P}\mathbb{A}(S_i), C = c_2)$, meaning that $P(S_i | \mathbb{P}\mathbb{A}(S_i))$ must change across domains. Also add variable θ_{S_i} in the graph, which points to S_i .

Step 2 (Determining edge direction with additional constraints) We then find v-structures in the graph and do orientation propagation, as in the PC algorithm [50], but we benefit from additional constraints implied by the augmented DAG structure. In this procedure, we first make use of the constraint that if variable S_i is adjacent to C , then there exists a θ variable, θ_{S_i} , pointing to S_i ; given this direction, one may further determine the directions of other edges [58]. In particular, suppose S_j is adjacent to S_i but not to C . Then if it is conditionally independent from C given a variable set that does not include S_i , orient the edge between them as $S_j \rightarrow S_i$; if it is conditionally independent from C given a variable set that includes S_i , orient it as $S_j \leftarrow S_i$. Second, if S_i and S_j are adjacent and are both adjacent to C , use the direction between them which gives independent changes in their conditional distributions, $P(S_i | \mathbb{P}\mathbb{A}(S_i))$ and $P(S_j | \mathbb{P}\mathbb{A}(S_j))$ [20]. If the changes are dependent in both directions, merge S_i and S_j as (part of) a “supernode” in the graph, and merge their corresponding θ variables.

Step 3 (Instantiating a DAG) Step 2 produces a partially directed acyclic graph (PDAG), representing an Markov equivalence class [54]. All augmented DAGs in this equivalence class have the same (conditional) independence relations, so finally, we instantiate from the equivalence class a DAG over Y and the variables in its MB. (It was shown in Section 2.3 that inferring the posterior of Y involves only the conditional distributions of Y and its children, not necessarily the conditional distribution of every feature.)

Two remarks are worth making on this procedure. First, to avoid strong assumptions on the forms of the conditional distributions, we make use of a nonparametric test of conditional independence, namely, kernel-based conditional independence test [59], when learning the augmented DAG. Second, given that the final inference for Y in the target domain, given by (3), depends only on the conditional distributions of Y and its children, one may extend some form of local graph structure discovery procedure (see, e.g., [8, 14]), to directly find the local graph structure involving Y and variables in its MB. This will be particularly beneficial on the computational load if we deal with high-dimensional features.

3.2 Latent-Variable CGAN for Modeling Changing Conditional Distributions

The second practical issue to be addressed is how to represent and learn the conditional distributions involved in (3). In light of the power of the Generative Adversarial Network (GAN) [17] in capturing the property of high-dimensional distributions and generating new random samples and the capacity of Conditional GAN (CGAN) [42] in learning flexible conditional distribution, we propose an extension of CGAN, namely, Latent-Variable CGAN (LV-CGAN), to model and learn a class of conditional distributions $P(S_i | \mathbb{P}\mathbb{A}(S_i), \theta_{S_i})$, with θ_{S_i} as a latent variable.

As an example, Figure 4 shows the structure of the LV-CGAN to model the conditional distribution of $P(X_3 | Y, X_2)$ across domains implied by the augmented DAG given in Figure 1. The whole network, including its parameters, is shared, and only the value of θ_3 may vary across domains. Hence, it explicitly models both changing and invariant

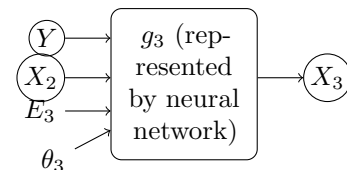


Figure 4: LV-CGAN for modeling $P(X_3 | Y, X_2, \theta_3)$ implied by the graph given in Figure 1.

portions in the conditional distribution; the former is captured by different values of θ_3 across domains, and the latter is implied by the fact that the whole network except the value of θ_3 is shared across domains. In the i th domain, θ_3 takes value $\theta_3^{(i)}$ and encodes the domain-specific information. The network specifies a model distribution $Q(X_3|Y, X_2, \theta_3)$ by the generative process

$$X_3 = g_3(Y, X_2, E_3, \theta_3), \quad (4)$$

which transforms random noise E_3 to X_3 , conditioning on Y , X_2 , and θ_3 . E_3 is independent of Y and X_2 , and its distribution is fixed (we used the standard Gaussian distribution). g_3 is a function represented by a neural network (NN) and shared by all domains. $Q(X_3|Y, X_2, \theta_3^{(i)})$ is trained to approximate the conditional distribution $P(X_3|Y, X_2)$ in the i th domain. For invariant conditional distributions such as $P(X_5|Y)$ in Figure 1, the θ input vanishes and it becomes a CGAN.

To estimate the LV-CGAN as well as the θ values, for which an example is (4), from empirical data, we adopt the adversarial training strategy [17, 25], which minimizes the distance between the empirical distributions in all source domains and the empirical distribution of the data sampled from model (4). Note that the θ variables are independent and, as a consequence, we can learn the LV-CGAN for each conditional distribution separately. It is clear that the values of the θ variables are not uniquely identifiable, but any estimated value would suffice as long as the conditional distributions across domains are properly modeled.

For the brevity of notation, suppose we aim to learn the conditional distribution $P(W|U, \theta)$, where U is the parent set of W ; then the corresponding LV-CGAN generative process is $W = g(U, E, \theta)$. For the example given in Figure 4, W , U , E , and θ correspond to X_3 and (Y, X_2) , E_3 , and θ_3 , respectively. Because our model involves an unknown θ variable whose distribution is unknown, we cannot directly sample data from the model. To enable adversarial training, we reparameterize θ by a linear transformation of the one-hot representation $\mathbf{1}_i$ of domain index i , i.e., $\theta = \Theta^\top \mathbf{1}_i$, where Θ can be learned by adversarial training.

We aim to match distributions in all source domains. In particular, in the i th source domain, we estimate the model by matching the joint distributions $P_{WU}^{(i)}$ and $Q_{WU}^{(i)}$, where $Q_{WU}^{(i)}$ is the joint distribution of the LV-CGAN output $W = g(U, E, \theta)$ and input U . Specifically, we use the Maximum Mean Discrepancy (MMD) [21, 48, 25] to measure the distance between the true and model distributions:

$$J^{(i)} = \left\| E_{(W,U) \sim P_{WU}^{(i)}} [\phi(W) \otimes \psi(U)] - E_{(W,U) \sim Q_{WU}^{(i)}} [\phi(W) \otimes \psi(U)] \right\|_{\mathcal{H}_w \otimes \mathcal{H}_u}^2, \quad (5)$$

where \mathcal{H}_w denotes a characteristic Reproducing Kernel Hilbert Space (RKHS) on the input feature space \mathcal{W} associated with a kernel $k(\cdot, \cdot) : \mathcal{W} \times \mathcal{W} \rightarrow \mathbb{R}$, ϕ the associated mapping such that $\phi(w) \in \mathcal{H}_w$, and \mathcal{H}_u the RKHS on the label space \mathcal{U} associated with kernel $l(\cdot, \cdot) : \mathcal{U} \times \mathcal{U} \rightarrow \mathbb{R}$ and mapping ψ . In practice, given a mini-batch of size n consisting of $\{(w_j^{(i)}, u_j^{(i)})\}_{j=1}^n$ sampled from the source domain data and $\{(\hat{w}_q^{(i)}, \hat{u}_q^{(i)})\}_{q=1}^n$ sampled from the generator, we need to estimate the empirical MMD for gradient evaluation and optimization:

$$\hat{J}^{(i)} = \frac{1}{n^2} \sum_j^n \sum_q^n k(w_j^{(i)}, w_q^{(i)}) l(u_j^{(i)}, u_q^{(i)}) - \frac{2}{n^2} \sum_j^n \sum_q^n k(w_j^{(i)}, \hat{w}_q^{(i)}) l(u_j^{(i)}, \hat{u}_q^{(i)}) + \frac{1}{n^2} \sum_j^n \sum_q^n k(\hat{w}_j^{(i)}, \hat{w}_q^{(i)}) l(\hat{u}_j^{(i)}, \hat{u}_q^{(i)}).$$

Given s source domains, we learn all parameters in the neural network g and $\{\theta^{(i)}\}_{i=1}^s$ by minimizing the total cost $\sum_{i=1}^s \hat{J}^{(i)}$. Clearly θ is not identifiable from the empirical data; for instance, for any invertible function h , we can change θ to $\theta' = h(\theta)$ and change the LV-CGAN $W = g(U, E, \theta)$ to $W = g(U, E, h^{-1}(\theta'))$ at the same time, while they imply the same conditional distribution of W given U across domains. The non-identifiability of θ is not our concern. It suffices as long as the conditional distributions across domains are properly modeled.

In the single-source setting, we assume $P(Y)$ does not change, and learn LV-CGAN on both source and target domains. We match the conditional in the source domain (as in the multiple-source case) and $P(X)$ in the target domain (as it has only unlabeled data) to learn LV-CGAN and domain-specific values of θ

We note that in the causality field, some recent methods represent functional causal models using neural networks [18], and leverage different complexities of the factorizations of a fixed data distribution in different directions to learn causal direction. In contrast, our LV-CGAN aims to encode the difference in the conditional distribution across domains, as indicated by different values of θ .

3.3 Inference on the Graphical Models

Finally, to apply the inference rule (3), which gives the posterior of Y in the target domain, we need make use of the marginal distributions $P(\theta_{V_j})$ and conditional distributions \mathcal{C}_{jk} , given in (2), for each V_j that is Y or any of its children. For the former, we use a smoothed version of the estimated values in the source domains, $\hat{\theta}_{V_j}^{(1)}, \dots, \hat{\theta}_{V_j}^{(s)}$. That is, a prior $p(\theta_{V_j})$ is obtained using kernel density estimation: $\hat{P}(\theta_{V_j} = a) = \frac{1}{s} \sum_{i=1}^s K_h(a - \hat{\theta}_{V_j}^{(i)})$, where K_h is the Gaussian kernel. We use Silverman’s rule of thumb to set the kernel width [47].

For the latter, one need estimate the conditional distribution implied by the LV-CGAN. We use a straightforward procedure based on sampling and kernel density estimation to estimate the conditional distribution $\mathcal{C}_{jk} = P(V_j = v_{jk}^\tau | \mathbb{P}\mathbb{A}(v_{jk}^\tau), \theta_{V_j})$. To this end, in the LV-CGAN corresponding to this conditional distribution, we let $\mathbb{P}\mathbb{A}(V_j)$ take its k th value in the target domain, and for each value of θ_{V_j} , we generate a number of random samples for V_j by sampling random points from $Q(E_{V_j})$ and feed them into the LV-CGAN. (In our experiments we used 100 random samples.) The (conditional) distribution of V_j is then estimated by kernel density estimation from these 100 samples.

Now all quantities involved in inference rule (3), including the structure of the augmented DAG over Y and the members of its MB, the prior distribution of the relevant θ variables, and the conditional distributions \mathcal{C}_{jk} , are available. One can then apply the rule to find the posterior of Y for the k th point in the target domain.

Regarding the computational complexity of the whole algorithm, the complexity of graph learning (a modification of the PC algorithm) is generally polynomial in the dimensionality, but it will roughly depend on the size of the Markov blanket of Y if one uses a suitable local structure learning method; the complexity of the inference phase is linear in the size of the Markov blanket, but in practice it might be costly because of sampling, and improving its efficiency in light of recent advances in Bayesian inference is under exploration.

4 Simulations

We simulated binary classification data from the graph on Figure 1, where we varied the number of source domains between 2, 4 and 9. We modeled each module in the graph with 1-hidden-layer MLPs. In each replication, we randomly sampled the MLP parameters and domain-specific θ values from $N(0, \mathbf{I})$. We sampled 500 points in each source domain and the target domain. We compared our approach, denoted by `Infer` against alternatives. We include a hypothesis combination method, denoted `simple_adapt` [33], linear mixture of source conditionals [57] denoted by `weigh_sample` and `comb_classif` respectively. We also compare to the pooling SVM (denoted `pool_SVM`), which merges all source data to train the SVM, as well as domain-invariant component analysis (DICA) [34], and Learning marginal predictors (LMP) [4]. The results are presented in Table 1. From the results, it can be seen that the proposed method outperforms the baselines by a large margin. Regarding significance of the results, we compared our method with the two other most powerful methods (DICA and LMP) using Wilcoxon signed rank test. The the p-values are 0.074, 0.009, 0.203 (against DICA) and 0.067, 0.074, 0.074 (against LMP), for 2, 4, and 9 source domains, respectively.

	DICA	weigh_sample	simple_adapt	comb_classif	LMP	pool_SVM	Infer
9 sources	80.04(15.5)	72.1(14.5)	70.0(14.3)	72.34(16.24)	78.90(13.81)	71.8(11.43)	83.90(9.02)
4 sources	74.16(13.2)	67.88(13.7)	65.22(16.00)	69.64(15.8)	79.06(13.93)	70.08(12.25)	85.38(11.31)
2 sources	86.56(13.63)	75.04(18.8)	69.42(17.87)	74.28(18.2)	84.52(13.72)	83.84(13.7)	93.10(7.17)

Table 1: Accuracy on simulated datasets for the baselines and proposed method. The values presented are averages over 10 replicates for each experiment. Standard deviation is in parentheses.

	DICA	weigh_sample	simple_adapt	comb_classif	LMP	pool_SVM	Infer
t2, t3 \rightarrow t1	29.32(2.5)	43.71(3.02)	38.53(2.6)	35.29(3.3)	46.8(1.3)	40.25(1.6)	64.22(5.2)
t1, t3 \rightarrow t2	24.5(3.6)	38.19(1.9)	35.87(2.8)	36.98(1.2)	39.11(2.1)	48.7(1.8)	66.75(6.0)
t1, t2 \rightarrow t3	21.7(3.9)	36.03(1.85)	35.1(1.5)	36.31(1.5)	39.28(2.05)	40.46(1.4)	74.05(2.7)

Table 2: Accuracy on the Wi-Fi data. The values presented are averages over 10 replicates for each experiment. Standard deviation is in parentheses.

5 Results on Real Data

5.1 MNIST-USPS

Here we use MNIST-USPS dataset to demonstrate whether LV-CGAN can successfully learn distribution changes and generate new domains. We also test the classification accuracy in the target domain. MNIST and USPS are two digit recognition datasets with 10 classes. We used $Y \rightarrow X$ (as in previous work such as [16]), where X is the image, as the graph for adaptation. There exists a slight scale change between the two domains. In this task there is only a single source domain, so we make some modification of the proposed approach to accommodate the single source setting. Specifically, we assume $P(Y)$ does not change and match the marginal distribution of generated images from LV-CGAN to that of the target domain images.

Following CoGAN [27, 5], we use the standard training-test splits for both MNIST and USPS. We compare our method with CORAL [53], DAN [28], DANN [12], DSN [5], and CoGAN [27]. We adopt the discriminator in CoGAN for classification by training on the generated labeled images from our proposed model, and choose baselines according to [27]. The quantitative results are shown in Table 3. It can be seen that our method achieves slightly better performance than CoGAN and outperforms the other methods.

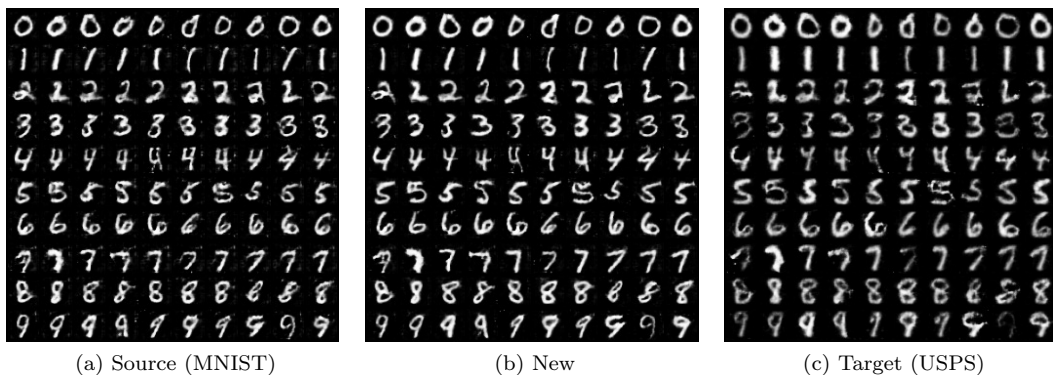


Figure 5: Generated images in the source, new, and target domain.

In addition, we provide qualitative results to demonstrate our model’s ability to generate new domains. As shown in Figure 5, we generate a new domain in the middle of MNIST and USPS. The images on the new domain have slightly larger scale than those on MNIST and slightly smaller scale than those on USPS, indicating that our model understands how the distribution changes.

Table 3: Comparison of different methods on MNIST-USPS.

CORAL	DAN	DANN	DSN	CoGAN	Infer
81.7	81.1	91.3	91.2	95.7	95.9

Although the slight scale change is not easily distinguishable by human eyes, it causes a performance degradation in terms of classification accuracy. The proposed LV-CGAN successfully recovers the joint distribution in the target domain and enables accurate prediction in the target domain.

5.2 Wi-Fi Localization Dataset

We then perform evaluations on the cross-domain indoor WiFi location dataset [61]. The WiFi data were collected from a building hallway area, which was discretized into a space of grids. At each grid point, the strength of WiFi signals received from D access points was collected. We aim to predict the location of the device from the D -dimensional WiFi signals.

For the multiple-source setting, we cast it as a classification problem, where each location is assigned with a discrete label. We only consider the task of transfer between different time periods, because the distribution of signal strength changes with time while the underlying graphical model is rather stable, which satisfies our model assumption. The WiFi data were collected by the same device during three different time periods t_1 , t_2 , and t_3 in the same hallway. Three sub-tasks including $t_2, t_3 \rightarrow t_1$, $t_1, t_3 \rightarrow t_2$, and $t_1, t_2 \rightarrow t_3$ are taken for performance evaluation. We thus obtained 19 possible labels, and in each domain we sampled 700 points in 10 replicates. We learn the graphical model, changing modules, and the LV-CGAN from the two source domains, and perform Bayesian inference in the target domain. The graph learned from the Wifi t_1 and t_2 data is given in Figure 6. We implement our LV-CGAN by using Multi-Layer Perceptions (MLPs) with one hidden layer (32 nodes) to model the function of each module and set the dimension of input noise E and θ involved in each module to 1. The reported result is classification accuracy of location labels. We used the same baselines as in the simulated dataset, and we present the results in Table 2. The results show that our method outperforms all baselines by a large margin.

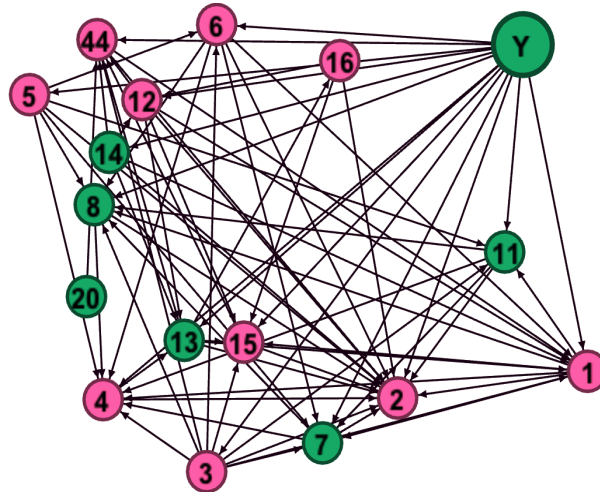


Figure 6: The causal structure learned by CD-NOD on the WiFi t_1 and t_2 datasets. Pink nodes denote the changing modules and green ones denote the constant modules whose conditional distribution does not change across domains.

6 Conclusion and Discussions

In this paper we proposed a framework to deal with unsupervised domain adaptation with multiple source domains by considering domain adaptation as an inference problem on a particular type of graphical model over the target variable and features or their combinations as super-nodes, which encodes the change properties of the data across domains. The graphical model can be directly estimated from data, leading to an automated, end-to-end approach to domain adaptation. As future work, we will study how the sparsity level of the learned graph affects the final prediction performance and, more importantly, aim to improve the computational efficiency of the method by resorting to more efficient inference procedures. Dealing with transfer learning with different feature spaces (known as heterogeneous transfer learning) by extending our approach is also a direction to explore.

References

- [1] M. Baktashmotlagh, M.T. Harandi, B.C. Lovell, and M. Salzmann. Unsupervised domain adaptation by domain invariant projection. In *ICCV 2013*, pages 769–776, Dec 2013.
- [2] E. Bareinboim, J. Tian, and J. Pearl. Recovering from selection bias in causal and statistical inference. In *Proc. 28th AAAI Conference on Artificial Intelligence*, pages 2410–2416, 2014.
- [3] S. Ben-David, S. Shalev-Shwartz, and Ruth Uner. Domain adaptation—can quantity compensate for quality? In *ISAIM 2012*, 2012.
- [4] G. Blanchard, G. Lee, and C. Scott. Generalizing from several related classification tasks to a new unlabeled sample. In *NIPS 2011*, pages 2178–2186, 2011.
- [5] Konstantinos Bousmalis, George Trigeorgis, Nathan Silberman, Dilip Krishnan, and Dumitru Erhan. Domain separation networks. In *Advances in Neural Information Processing Systems*, pages 343–351, 2016.
- [6] R. Chattopadhyay, J. Ye, S. Panchanathan, W. Fan, and I. Davidson. Multi-source domain adaptation and its application to early detection of fatigue. In *KDD*, 2011.
- [7] Q. Chen, Y. Liu, Z. Wang, I. Wassell, and K. Chetty. Re-weighted adversarial adaptation network for unsupervised domain adaptation. In *Proceedings of the IEEE Conference on Computer Vision and Pattern Recognition*, pages 7976–7985, 2018.
- [8] G. F. Cooper. A simple constraint-based algorithm for efficiently mining observational databases for causal relationships. *Data Mining and Knowledge Discovery*, 1:203–224, 1997.
- [9] C. Cortes, Y. Mansour, and M. Mohri. Learning bounds for importance weighting. In *NIPS 23*, 2010.
- [10] N. Courty, R. Flamary, A. Habrard, and A. Rakotomamonjy. Joint distribution optimal transportation for domain adaptation. In *NIPS*, 2017.
- [11] L. Duan, I. W. Tsang, D. Xu, and T. S. Chua. Domain adaptation from multiple sources via auxiliary classifiers. In *ICML*, 2009.
- [12] Y. Ganin, E. Ustinova, H. Ajakan, P. Germain, H. Larochelle, F. Laviolette, M. Marchand, and V. Lempitsky. Domain-adversarial training of neural networks. *Journal of Machine Learning Research*, 17(1):2096–2030, 2016.
- [13] J. Gao, W. Fan, J. Jiang, and J. Han. Knowledge transfer via multiple model local structure mapping. In *International Conference on Knowledge Discovery and Data Mining, Las Vegas, NV*, 2008.
- [14] T. Gao and Q. Ji. Local causal discovery of direct causes and effects. In *NIPS’15*, pages 2503–2511, 2015.

- [15] B. Gong, K. Grauman, and F. Sha. Connecting the dots with landmarks: Discriminatively learning domain-invariant features for unsupervised domain adaptation. In *ICML*, pages 222–230, 2013.
- [16] M. Gong, K. Zhang, T. Liu, D. Tao, C. Glymour, and B. Schölkopf. Domain adaptation with conditional transferable components. In *Proceedings of the 33rd International Conference on Machine Learning (ICML 2016)*, volume 48, pages 2839–2848, 2016.
- [17] I. Goodfellow, J. Pouget-Abadie, M. Mirza, B. Xu, D. Warde-Farley, S. Ozair, A. Courville, and Y. Bengio. Conditional generative moment-matching networks. In *NIPS*, pages 2672–2680, 2014.
- [18] O. Goudet, D. Kalainathan, P. Caillou, D. Lopez-Paz, I. Guyon, M. Sebag, A. Tritas, and P. Tubaro. Learning functional causal models with generative neural networks. *arXiv preprint arXiv:1709.05321*, 2017.
- [19] A. Gretton, K. M. Borgwardt, M. J. Rasch, B. Schölkopf, and A. Smola. A kernel two-sample test. *JMLR*, 13:723–773, 2012.
- [20] B. Huang, K. Zhang, J. Zhang, R. Sanchez Romero, C. Glymour, and B. Schölkopf. Behind distribution shift: Mining driving forces of changes and causal arrows. In *ICDM 2017*, 2017.
- [21] J. Huang, A. Smola, A. Gretton, K. Borgwardt, and B. Schölkopf. Correcting sample selection bias by unlabeled data. In *NIPS 19*, pages 601–608, 2007.
- [22] A. Iyer, A. Nath, and S. Sarawagi. Maximum mean discrepancy for class ratio estimation: Convergence bounds and kernel selection. In *Proc. ICML 2014*, 2014.
- [23] D. Koller and N. Friedman. *Probabilistic Graphical Models: Principles and Techniques*. MIT Press, Cambridge, MA, 2009.
- [24] S. Lauritzen and T. Richardson. Chain graph models and their causal interpretations. *Journal of the Royal Statistical Society: Series*, 63:321–36, 2002.
- [25] Yujia Li, Kevin Swersky, and Rich Zemel. Generative moment matching networks. In *ICML*, pages 1718–1727, 2015.
- [26] Z. C. Lipton, Y. Wang, and A. Smola. Detecting and correcting for label shift with black box predictors. *arXiv preprint arXiv:1802.03916*, 2018.
- [27] Ming-Yu Liu and Oncl Tuzel. Coupled generative adversarial networks. In *Advances in neural information processing systems*, pages 469–477, 2016.
- [28] M. Long, Y. Cao, J. Wang, and M. Jordan. Learning transferable features with deep adaptation networks. In *ICML-15*, pages 97–105, 2015.
- [29] M. Long, J. Wang, G. Ding, J. Sun, and P. S. Yu. Transfer feature learning with joint distribution adaptation. In *Proceedings of the IEEE international conference on computer vision*, pages 2200–2207, 2013.
- [30] M. Long, H. Zhu, J. Wang, and M. I. Jordan. Deep transfer learning with joint adaptation networks. In *Proc. 34th International Conference on Machine Learning (ICML 2017)*, 2017.
- [31] T. Liu D. Tao C. Glymour M. Gong, K. Zhang and B. Schölkopf. Domain adaptation with conditional transferable components. In *ICML 2016*, 2016.
- [32] S. Magliacane, T. van Ommen, T. T. Claassen, S. Bongers, P. Versteeg, and J. M. Mooij. Domain adaptation by using causal inference to predict invariant conditional distributions. In *NIPS*, 2018.
- [33] Y. Mansour, M. Mohri, and A. Rostamizadeh. Domain adaptation with multiple sources. In *NIPS 19*, pages 1041–1048, Cambridge, MA, 2008. MIT Press.
- [34] K. Muandet, D. Balduzzi, and B. Schölkopf. Domain generalization via invariant feature representation. In *Proceedings of the 30th International Conference on Machine Learning, JMLR: W&CP Vol. 28*, 2013.

- [35] S. J. Pan, I. W. Tsang, J. T. Kwok, and Q. Yang. Domain adaptation via transfer component analysis. *IEEE Transactions on Neural Networks*, 22:199–120, 2011.
- [36] E. Pearl and E. Bareinboim. Transportability of causal and statistical relations: A formal approach. In *AAAI 2011*, pages 247–254, 2011.
- [37] J. Pearl. *Probabilistic Reasoning in Intelligent Systems: Networks of Plausible Inference*. Morgan Kaufmann, 1988.
- [38] J. Pearl. *Causality: Models, Reasoning, and Inference*. Cambridge University Press, Cambridge, 2000.
- [39] J. Pearl and E. Bareinboim. Transportability of causal and statistical relations: A formal approach. In *Proc. AAAI 2011*, pages 247–254, 2011.
- [40] Judea Pearl. A probabilistic calculus of actions. In *UAI 1994*, pages 454–462, 1994.
- [41] M. D. Plessis and M. Sugiyama. Semi-supervised learning of class balance under class-prior change by distribution matching. In *ICML-12*, pages 823–830, 2012.
- [42] Y. Ren, J. Li, Y. Luo, and J. Zhu. Generative adversarial nets. In *NIPS*, pages 2928–2936, 2016.
- [43] P. R. Rosenbaum and D. B. Rubin. The central role of the propensity score in observational studies for causal effects. *Biometrika*, 70:41–55, 1983.
- [44] M.T. Rosenstein, Z. Marx, L.P. Kaelbling, and T.G. Dietterich. To transfer or not to transfer. In *NIPS 2005 Workshop on Inductive Transfer: 10 Years Later*, 2005.
- [45] B. Schölkopf, D. Janzing, J. Peters, E. Sgouritsa, K. Zhang, and J. Mooij. On causal and anticausal learning. In *ICML-12*, Edinburgh, Scotland, 2012.
- [46] H. Shimodaira. Improving predictive inference under covariate shift by weighting the log-likelihood function. *Journal of Statistical Planning and Inference*, 90:227–244, 2000.
- [47] B. W. Silverman. *Density Estimation for Statistics and Data Analysis*. London: Chapman & Hall/CRC, 1986.
- [48] L. Song, K. Fukumizu, and A. Gretton. Kernel embeddings of conditional distributions. *IEEE Signal Processing Magazine*, 30:98 – 111, 2013.
- [49] P. Spirtes, C. Glymour, and R. Scheines. *Causation, Prediction, and Search*. Springer-Verlag Lectures in Statistics, 1993.
- [50] P. Spirtes, C. Glymour, and R. Scheines. *Causation, Prediction, and Search*. MIT Press, Cambridge, MA, 2nd edition, 2001.
- [51] A. Storkey. When training and test sets are different: Characterizing learning transfer. In J. Candela, M. Sugiyama, A. Schwaighofer, and N. Lawrence, editors, *Dataset Shift in Machine Learning*, pages 3–28. MIT Press, 2009.
- [52] M. Sugiyama, T. Suzuki, S. Nakajima, H. Kashima, P. von Bünaui, and M. Kawanabe. Direct importance estimation for covariate shift adaptation. *Annals of the Institute of Statistical Mathematics*, 60:699–746, 2008.
- [53] Baochen Sun and Kate Saenko. Deep coral: Correlation alignment for deep domain adaptation. In *European Conference on Computer Vision*, pages 443–450. Springer, 2016.
- [54] T. Verma and . Pearl. Equivalence and synthesis of causal models. In *UAI 1990*, pages 255–270, 1991.
- [55] S. Xie, Z. Zheng, L. Chen, and C. Chen. Learning semantic representations for unsupervised domain adaptation. In *ICML-18*, volume 80, pages 5423–5432, 2018.
- [56] B. Zadrozny. Learning and evaluating classifiers under sample selection bias. In *ICML-04*, pages 114–121, Banff, Canada, 2004.

- [57] K. Zhang, M. Gong, and B. Schölkopf. Multi-source domain adaptation: A causal view. In *Twenty-Ninth AAAI Conference on Artificial Intelligence*, 2015.
- [58] K. Zhang, B. Huang, J. Zhang, C. Glymour, and B. Schölkopf. Causal discovery from non-stationary/heterogeneous data: Skeleton estimation and orientation determination. In *IJCAI*, volume 2017, page 1347, 2017.
- [59] K. Zhang, J. Peters, D. Janzing, and B. Schölkopf. Kernel-based conditional independence test and application in causal discovery. In *UAI 2011*, 2011.
- [60] K. Zhang, B. Schölkopf, K. Muandet, and Z. Wang. Domain adaptation under target and conditional shift. In *ICML-13*, 2013.
- [61] Kai Zhang, V. Zheng, Q. Wang, J. Kwok, Q. Yang, and I. Marsic. Covariate shift in hilbert space: A solution via surrogate kernels. In *Proceedings of the 30th International Conference on Machine Learning*, pages 388–395, 2013.